Electronic excitations in the correlated metal $BaV_{0.98}Ti_{0.02}S_3$ studied using resonant inelastic soft x-ray scattering

2010 J. Phys.: Condens. Matter 22 025504

(http://iopscience.iop.org/0953-8984/22/2/025504)

J. Phys.: Condens. Matter **22** (2010) 025504 (5pp) doi:10.1088/0953-8984/22/2/025504

Electronic excitations in the correlated metal $BaV_{0.98}Ti_{0.02}S_3$ studied using resonant inelastic soft x-ray scattering

T Learmonth[1], P-A Glans[1], J-H Guo[2], M Greenblatt[3] and K E Smith[1]

[1] Department of Physics, Boston University, 590 Commonwealth Avenue, Boston, MA, USA
[2] Advanced Light Source, Lawrence Berkeley National Laboratory, Berkeley, CA, USA
[3] Department of Chemistry and Chemical Biology, Rutgers University, Piscataway, NJ, USA

Received 20 August 2009, in final form 31 October 2009
Published 14 December 2009
Online at stacks.iop.org/JPhysCM/22/025504

Abstract

Electronic excitations in the correlated metal $BaTi_{0.02}V_{0.98}S_3$ have been studied using resonant inelastic soft x-ray scattering at the V L edge. The *intensities* of the intra-atomic d–d* excitations and the elastic x-ray scattering feature are found to be temperature dependent, with the intensity increasing with decreasing temperature until saturation is reached near 100 K. The behavior of the spectral features is interpreted as evidence of a shift in the 3d electrons from more band-like states at higher temperature to more localized states at low temperature.

(Some figures in this article are in colour only in the electronic version)

$BaVS_3$ is a complex quasi-one-dimensional (1D) correlated metal that displays the effects of competing orbital, spin, lattice, and electronic interactions [1, 2]. It undergoes three phase transitions below room temperature. One of these transitions, a metal-to-insulator transition at 70 K, is of particular interest. It coincides with a cusp-like maximum in the magnetic susceptibility that signals the formation of spin singlets [3, 4], but not the onset of long range magnetic order [5]. Structural studies have indicated that the metal-to-insulator transition coincides with a doubling of the unit cell along the 1D axis, and, due to the presence of two V sites in each undoubled unit cell, the formation of four inequivalent V sites [2, 6]. Further work suggests that the magnetic and transport properties of $BaVS_3$ could be explained by an equal population of two types of states at the Fermi energy (E_F), one narrow pair of states and one more extended state that forms a broad band along the 1D axis. This broad band would then form a charge density wave (CDW) at the metal-to-insulator transition. However, anomalous x-ray scattering has detected no such CDW, leading to the suggestion that the CDW could coincide with an out of phase charge ordering on the narrow bands, leaving minimal overall charge disproportionation [7, 8]. The result is a state that is more orbitally ordered than charge ordered. Thus the metal-to-insulator transition in $BaVS_3$ is complex, and dependent on the equilibrium found between spin, orbital, lattice, and quasi-one-dimensional instabilities. $BaVS_3$ is nominally $3d^1$, but Ti can be substituted for V to introduce $3d^0$ sites. For Ti concentrations above 5% ($x > 0.05$), $BaTi_xV_{1-x}S_3$ is a paramagnetic semiconductor from 4.2 to 300 K, and the cusp in the magnetic susceptibility associated with the metal-to-insulator transition vanishes [3]; both observations are plausibly explained in terms of unpaired spins and Anderson localization caused by the Ti sites. However, for $x = 0.02$, diffuse x-ray scattering did not display the CDW associated with the metal–insulator transition in pure $BaVS_3$, but rather revealed a different structural 'pseudo-transition' at 250 K rather than 70 K [9]. Transport measurements of $BaTi_xV_{1-x}S_3$ for $x < 0.05$ have not been made, so the nature of this pseudo-transition is uncertain. However, Fagot *et al* suggest that it could correspond to a CDW with a different wavevector [9].

Measurements of bulk properties such as transport and magnetic susceptibility can be sensitive to effects that are not representative of the local electronic structure which appears to play an important role in $BaVS_3$. Consequently, measurements of the more local interactions in $BaTi_xV_{1-x}S_3$ are desirable to help elucidate the changes observed with Ti substitution in transport and magnetic susceptibility measurements. Resonant inelastic soft x-ray scattering (RIXS) is an ideal local probe of electronic structure in $BaTi_xV_{1-x}S_3$, due to the presence of a core hole in the intermediate state. RIXS is element, site, and

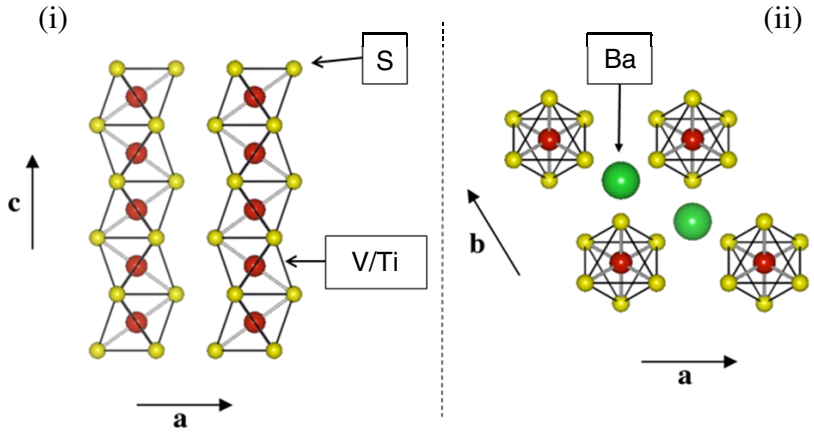

Figure 1. The crystal structure of $BaTi_xV_{1-x}S_3$. S sites are the smallest spheres, V/Ti sites are indicated by darker spheres enclosed by S sites, and Ba sites are the largest spheres. (i) VS_6 or TiS_6 octahedra are face sharing along the quasi-1D $\boldsymbol{c}$ axis. (ii) The resulting chains form a triangular pattern in the $\boldsymbol{ab}$ plane, with Ba sites at the centers.

orbital specific, and very sensitive to hybridization and d–d* electron excitations [10, 11].

We present here the results of a study of the electronic structure of single crystal $BaTi_{0.02}V_{0.98}S_3$ using RIXS and x-ray absorption spectroscopy (XAS). V L-edge XAS and RIXS were used as a function of both excitation energy and sample temperature to probe the local electronic structure. The XAS L-edge spectra show no change with sample temperature. However, L-edge RIXS spectra reveal low energy excitations that change spectral intensity as a function of sample temperature. The intensity of both the elastic scattering feature and the d–d* excitation feature increases dramatically upon cooling to 20 K, indicating an increase in the localization of the V 3d states. We discuss our data in the context of current models of the metal to non-metal transitions in $BaVS_3$.

The RIXS and XAS measurements were undertaken on the soft x-ray undulator beamline 7.0.1 at the Advanced Light Source, Lawrence Berkeley National Laboratory, which is equipped with a spherical grating monochromator. The $BaV_{0.98}Ti_{0.02}S_3$ single crystals were approximately 2–3 mm in length (along the quasi-1D $\boldsymbol{c}$ axis) and 0.5 mm along the perpendicular axes. Four crystals were aligned together to form a larger sample area, with the resulting crystal $\boldsymbol{c}$ axis in the scattering plane. The surface normal to the sample cluster was at a 70° angle to the incident photon beam, and as a result the incident photon electric field vector was nearly perpendicular to the sample $\boldsymbol{c}$ axis. RIXS measurements were made using a Nordgren-type, Rowland circle x-ray emission spectrometer [12], aligned at 90° to the incident photon beam, parallel to the incident photon electric field vector. For the RIXS measurements both the incident photon and the emission spectrometer energy resolutions were set to 0.5 eV at a photon energy of 530 eV. XAS measurements were taken in the total fluorescence yield (TFY) mode via a silicon diode and in the total electron yield (TEY) mode via the sample drain current, with a nominal incident photon resolution of 0.2 eV. The base pressure of the measurement chamber during the experiment was 2×10^{-10} Torr. The O K-edge emission was calibrated to metallic Zn $L_{\alpha 1,2}$ and $L_{\beta 1}$ emission lines in second order. All RIXS spectra are subject to the effects of self-absorption, where some portion of the emitted x-rays are re-absorbed by the sample. This effect can alter the *shape* of a measured RIXS spectrum if some of the emitted x-rays making up the spectrum have an energy high enough to resonantly create a second core hole [13]. Although self-absorption in our experiment was found to be small, we have corrected all of our emission spectra following the procedure published previously for $CaCu_3Ti_4O_{12}$ [14].

The room temperature crystal structure of $BaTi_xV_{1-x}S_3$ (see figure 1) consists of face sharing chains of VS_6 (or TiS_6) octahedra aligned along the $\boldsymbol{c}$ axis. These chains order hexagonally in the $\boldsymbol{ab}$ plane, with Ba sites in between [15]. The unit cell is hexagonal. Pure $BaVS_3$ undergoes a structural phase transition near 240 K that results in an orthorhombic cell. This distortion causes the transition metal sites to shift perpendicular to the $\boldsymbol{c}$ axis, producing zigzag rather than straight quasi-1D chains [16]. As well as the primary octahedral component, the ligand field has a trigonal component that splits the lower lying V 3d t_{2g} states further into a higher energy z^2 state that forms a ∼1 eV wide band and two lower energy, nearly degenerate e(t_{2g}) states [15]. At the metal-to-insulator transition in $BaVS_3$, the structural distortion breaks site symmetry along the $\boldsymbol{c}$ axis through the afore-mentioned tetramerization [6], and spin pairs form in the $\boldsymbol{ab}$ plane [4, 5]. In attaining the spin paired state, orbital ordering is thought to emerge which features alternating pairs of band-like z^2 and more localized e(t_{2g}) occupation [7, 8].

Figure 2 presents XAS spectra from $BaTi_{0.02}V_{0.98}S_3$ recorded in both the TEY and TFY modes. The XAS spectra measured in TFY are shown as dashed lines, while those measured in TEY are shown as solid lines. The top panel shows spectra recorded with the sample at room temperature, while the bottom panel shows spectra recorded with the sample at approximately 20 K. The first large spectral feature from 514 to 518 eV corresponds to the excitation of a V $2p_{3/2}$ core electron into the conduction band (L_3), and the second from 521 to 526 eV to the excitation of a V $2p_{1/2}$ core electron into the conduction band (L_2). The structure within the L_3

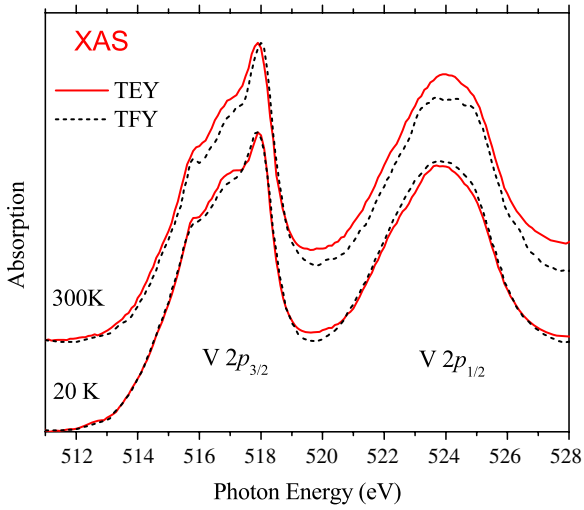

Figure 2. V L-edge XAS measurements of $BaTi_{0.02}V_{0.98}S_3$. The solid lines show the TEY spectra, and the dotted lines the TFY spectra. The top two spectra were collected at room temperature (300 K) and the bottom two at 20 K. The structure in the lower energy L_3 feature is multiplet dominated.

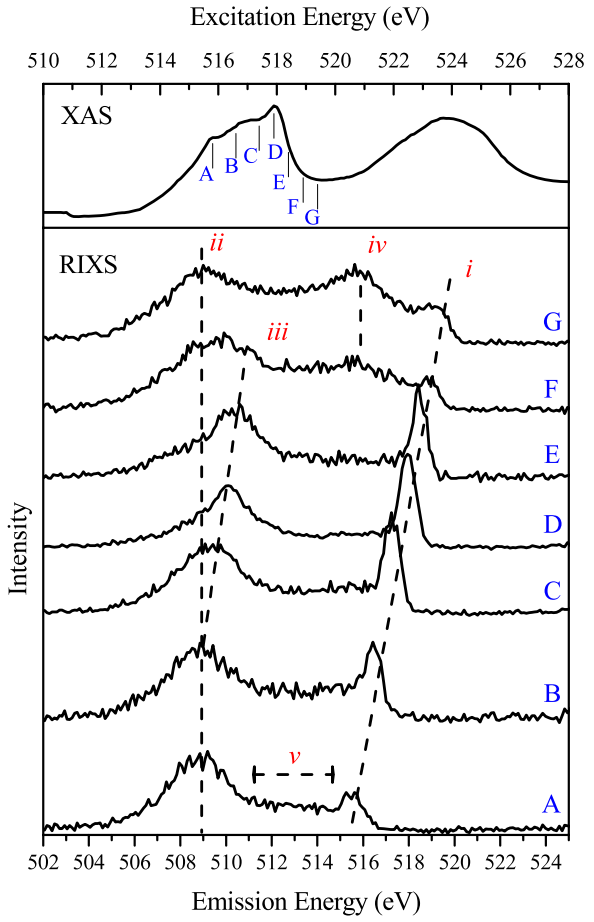

Figure 3. Bottom panel: room temperature V L-edge RIXS spectra from of $BaTi_{0.02}V_{0.98}S_3$ as a function of excitation energy. Top panel: room temperature TEY spectrum from figure 2, with the RIXS excitation energies marked A–G. The dashed lines i–iv correspond to features described in the text.

peak is similar to that observed in L-edge XAS from VO_2, which has the same formal valency as $BaVS_3$ but a different crystal structure [17]. This indicates that the measured XAS structure is due more to intrinsic V^{4+} multiplet effects rather than the conduction band density of states [18]. Such an interpretation is consistent with the fact that we measure no significant temperature dependence to the XAS spectra.

Figure 3 presents RIXS spectra recorded from $BaTi_{0.02}V_{0.98}S_3$ at room temperature as a function of excitation energy. Also shown in figure 3 is the corresponding TEY XAS spectrum from figure 2, where the energies used to excite the RIXS spectra are marked 'A' through 'G'. Four spectral features are clearly resolved in the RIXS spectra. The highest energy RIXS feature, labeled i, is due to elastic scattering. A second feature, labeled ii, appears at a nearly constant emission energy of about 509 eV. This fluorescence feature is due to the radiative transition of valence electrons into the L_3 core hole. A third feature, marked iii, is only visible in the above threshold excitation spectra (C–F), and appears at a constant energy loss of 7.8 eV below the excitation energy (i), placing it in the energy range of a charge transfer excitation. Such excitations have been observed in RIXS spectra recorded from VO_2 and NaV_2O_5, with formal valencies of $3d^1$ and $3d^{0.5}$ respectively [17]. However in these materials the charge transfer feature is most intense near the L-edge absorption onset, rather than at a higher energy XAS multiplet peak as observed here [17]. The intensity of feature iii in spectra D and E is such that it dwarfs the L_3 fluorescence (feature ii). Feature iv is visible in spectra G and H, lying at higher emission energy than feature iii; this is the onset of L_2 fluorescence. At excitation energies A through E, there is also substantial spectral weight between features i and ii, but no well defined peak. This spectral weight (between approximately 512–515 eV, marked v above spectrum A in figure 3) has little excitation energy dependence, and although it appears to decrease in intensity slightly in spectrum D, it is present in all of the RIXS spectra before feature iv emerges. The sample temperature dependence of this emission is discussed below.

The RIXS experiment reported in figure 3 for a room temperature sample was repeated at the same set of excitation energies from a sample held at 20 K. Only the spectra recorded at excitation energies A and B showed any change with sample temperature, with the most pronounced change observed at excitation energy A. Figure 4 presents a series of RIXS spectra taken at excitation energy A as a function of sample temperature between 20 and 300 K. The spectra in figure 4 are plotted as a function of energy loss ($h\nu_{out}$–$h\nu_{in}$). Each spectrum in figure 4 can be divided into three parts: the L_3 fluorescence feature at 7 eV (feature ii), the elastic feature at 0 eV (feature i), and the diffuse spectral weight between 4 and 1 eV (feature v). All spectra are normalized to the maximum intensity of feature ii. Examination of the spectra in figure 4 reveals that there is a shift in the loss energy of feature ii of approximately 0.5 eV toward higher emission energy with decreasing temperature. It is not clear if the change in energy of this feature with temperature is due to a shift of the entire feature or a change in spectral weight of unresolved

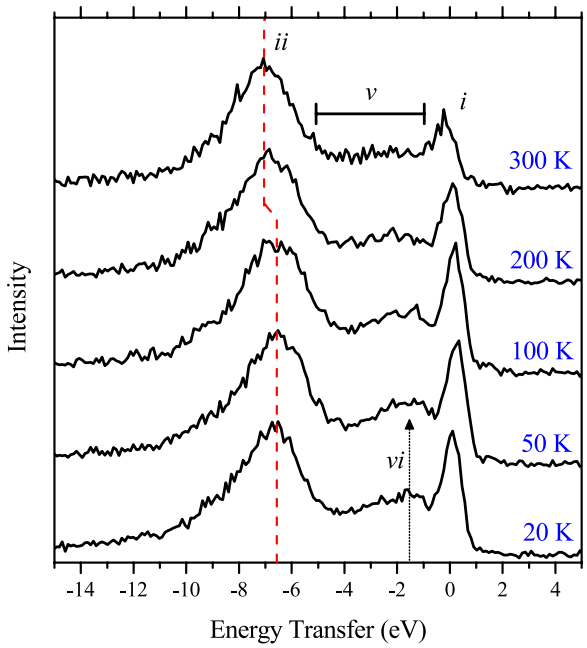

Figure 4. V L-edge RIXS with excitation energy A (see figure 3) is repeated as a function of temperature from 20 K (bottom spectrum) to 300 K (top spectrum). The features marked with dashed lines are described in the text.

components. As noted in figure 3, the room temperature spectrum contains little indication of a defined peak within feature v. However, upon cooling to 200 K, the first sign of a peak within feature v emerges. In the 100 K spectrum the peak becomes more clear, centered at approximately 1.8 eV (see arrow marked vi in figure 4). The increase in spectral weight with the emergence of feature vi is not accompanied with a decrease in spectral weight in feature v (with respect to feature ii), so it is not a shift in spectral weight. Along with the emergence of feature vi, the intensity of feature i increases to near parity with feature ii upon cooling from room temperature to 100 K. Between 100 and 50 K, the intensity of feature vi reaches a maximum, and finally the RIXS spectra change only minimally between 50 and 20 K.

To understand the RIXS spectra, we refer to dynamical mean-field based bandstructure calculations for $BaVS_3$ [8]. The symmetry adapted 3d orbitals are calculated to include a ∼1 eV wide A_{1g} orbital of primarily d_z^2 character (parallel to the 1D axis) that hybridizes strongly with the S 3p orbitals, and E_g states of mixed orbital character that hybridize only weakly [8]. These primarily 3d states occupy the energy range from E_F to about 1 eV below E_F. Between 1 and 3 eV, the bandstructure consists of strongly dispersing bands of primarily S 3p character, and below 3 eV mostly weakly dispersing bands, also primarily of S 3p character. From this picture we can assign the fluorescence-like features ii and iv to emission from the S 3p bands via hybridization with V 3d states. Soft x-ray emission has been shown to be highly sensitive to shallow core level and valence band hybridization [19]. Likewise, at least part of feature v can be assigned to emission from the more strongly dispersing S 3p bands hybridized with V 3d states. However, feature v also displays characteristics associated with an electronic excitation. A charge transfer-like excitation has been observed in optical conductivity measurements of $BaVS_3$ [20]. This excitation forms a broad feature from 1.0 to 3.0 eV [20]. It is not polarization dependent, and was attributed to an inter-atomic S 3p → V 3d excitation between strongly dispersing bands. This excitation is likely the origin of some of the spectral weight that forms feature v.

In considering the origin of feature vi (figure 4), it should be noted that the optical conductivity spectrum displays no temperature dependence above about 1 eV [20]. However, optical conductivity measures dipole allowed low energy excitations, and is insensitive to dipole forbidden d–d* excitations. Feature vi is in the correct energy range for an intra-atomic d–d* excitation, similar to those observed in other transition metal compounds [17, 21]. From the dynamical mean-field calculation, the e_g and A_{1g} states in $BaVS_3$ lie 1.5 eV above E_F, while the E_g states lie at E_F [8]. While it is likely that the intermediate RIXS state accessed in the spectra presented in figure 3 corresponds to the e_g and A_{1g} states, our experiment did not allow rotation of the sample, which would have helped distinguish the orbital character [11]. However, the ∼1.5 eV calculated crystal field separation is close to the 1.8 eV energy of feature vi, and we identify feature vi as an intra-atomic d–d* excitation.

The temperature dependence of the d–d* excitation and the relative increase in intensity of the elastic scattering suggest that there is a change in the electronic structure of $BaTi_{0.02}V_{0.98}S_3$ between 50 and 100 K. While a d–d* excitation is intrinsically a localized phenomenon, elastic scattering also has a local nature, since it corresponds to the direct intra-atomic recombination of the core excited electron. Both excitations share a RIXS intermediate state, but are the result of different RIXS final states. Since the elastic feature i corresponds to a RIXS final state identical to the ground state by definition, this suggests that a change in the *intermediate* state may be responsible for the simultaneous increase in intensity of the elastic scattering feature (i) and the d–d* excitation (vi). This in turn suggests that the intermediate RIXS state becomes increasingly localized with decreasing temperature. The cold temperature saturation of the RIXS features intensity occurs near 100 K, which is colder than that of the structural fluctuations observed in diffuse x-ray scattering from the $BaTi_{0.02}V_{0.98}S_3$ [9]. However, RIXS is sensitive to both changes in localization and changes in orbital ordering, so observations of spectral weight changes may be more suitable as indicators of an underlying transition rather than the transition's temperature

In conclusion, the local electronic structure of $BaTi_{0.02}V_{0.98}S_3$ was studied as a function of sample temperature using V L-edge XAS and RIXS. The XAS measurements reveal no changes in the unoccupied electronic structure with temperature. In contrast, the RIXS spectra reveal a significant temperature dependence to both the elastic and d–d* excitation features, with the intensity of both features increasing dramatically as the sample is cooled. This indicates an increase in the localization of the V 3d states at low temperatures.

Acknowledgments

The Boston University (BU) program is supported in part by the Department of Energy under DE-FG02-98ER45680. The ALS is supported by the US Department of Energy under Contract No. DE-AC02-05CH11231. TL acknowledges support from the ALS Doctoral Fellowship Program. Cormac McGuinness is thanked for numerous helpful comments.

References

[1] Mihály G, Kézsmárki I, Zámborszky F, Miljak M, Penc K, Fazekas P, Berger H and Forró L 2000 *Phys. Rev.* B **61** 7831
Nakamura M, Sekiyama A, Namatame H, Fujimori A, Yoshihara H, Ohtani T, Misu A and Takano M 1994 *Phys. Rev.* B **49** 16191
[2] Fagot S, Foury-Leylekian P, Ravy S, Pouget J-P and Berger H 2003 *Phys. Rev. Lett.* **90** 196401
[3] Matsuura K, Wada T, Nakamizo T, Yamauchi H and Tanaka S 1991 *Phys. Rev.* B **43** 13118
[4] Nakamura H, Imai H and Shiga M 1997 *Phys. Rev. Lett.* **79** 3779
[5] Nakamura H, Yamasaki T, Giri S, Imai H, Shiga M, Kojima K, Nishi M, Kakurai K and Metoki N 2000 *J. Phys. Soc. Japan* **69** 2763
[6] Fagot S, Foury-Leylekian P, Ravy S, Pouget J P, Anne M, Popov G, Lobanov M V and Greenblatt M 2005 *Solid State Sci.* **7** 718
[7] Fagot S, Foury-Leylekian P, Ravy S, Pouget J-P, Lorenzo E, Joly Y, Greenblatt M, Lobanov M V and Popov G 2006 *Phys. Rev.* B **73** 033102
[8] Lechermann F, Biermann S and Georges A 2005 *Phys. Rev. Lett.* **94** 166402
[9] Fagot S, Foury-Leylekian P, Pouget J-P, Popov G, Lobanov M, Greenblatt M and Fertey P 2006 *Physica* B **378** 1068
[10] Gel'mukhanov F and Agren H 1999 *Phys. Rep.* **312** 87
[11] Kuiper P, Guo J H, Sathe C, Nordgren J, Pothuizen J J M, de Groot F M F and Sawatzky G A 1998 *Phys. Rev. Lett.* **80** 5204
[12] Nordgren J and Nyholm R 1986 *Nucl. Instrum. Methods* A **246** 242
[13] Mueller D R, Ederer D L, van Ek J, O'Brien W L, Dong Q Y, Jia J J and Callcott T A 1996 *Phys. Rev.* B **54** 15034
Jimenez-Mier J, van Ek J, Ederer D L, Callcott T A, Jia J J, Carlisle J, Terminello L, Asfaw A and Perera R C 1999 *Phys. Rev.* B **59** 2649
[14] McGuinness C, Downes J E, Sheridan P, Glans P-A, Smith K E, Si W and Johnson P D 2005 *Phys. Rev.* B **71** 195111
[15] Massenet O, Since J J, Mercier J, Avignon M, Buder R and Nguyen V D 1979 *J. Phys. Chem. Solids* **40** 573
[16] Ghedira M, Chenavas J, Sayetat F, Marezio M, Massenet O and Mercier J 1981 *Acta Crystallogr.* B **37** 1491
[17] Schmitt T, Duda L C, Augustsson A, Guo J H, Nordgren J, Downes J E, McGuinness C, Smith K E, Dhalenne G, Revcolevschi A, Klemm M and Horn S 2002 *Surf. Rev. Lett.* **9** 1369
[18] Degroot F M F, Fuggle J C, Thole B T and Sawatzky G A 1990 *Phys. Rev.* B **42** 5459
de Groot F 2001 *Chem. Rev.* **101** 1779
[19] Glans P-A, Learmonth T, McGuinness C, Smith K E, Guo J, Walsh A, Watson G W and Egdell R G 2004 *Chem. Phys. Lett.* **399** 98
Payne D J, Egdell R G, Walsh A, Watson G W, Guo J, Glans P A, Learmonth T and Smith K E 2006 *Phys. Rev. Lett.* **96** 157403
[20] Kezsmarki I, Mihaly G, Gaal R, Barisic N, Akrap A, Berger H, Forro L, Homes C C and Mihaly L 2006 *Phys. Rev. Lett.* **96** 186402
[21] Butorin S M, Guo J H, Wassdahl N and Nordgren E J 2000 *J. Electron Spectrosc. Relat. Phenom.* **110** 235
Kotani A and Shin S 2001 *Rev. Mod. Phys.* **73** 203